

# Regression of advanced rat and human gliomas by local or systemic treatment with oncolytic parvovirus H-1 in rat models

Karsten Geletneky, Irina Kiprianova, Ali Ayache, Regina Koch, Marta Herrero y Calle, Laurent Deleu, Clemens Sommer, Nadja Thomas, Jean Rommelaere<sup>†</sup>, and Jörg R. Schlehofer<sup>†</sup>

*Department of Neurological Surgery, University of Heidelberg, Heidelberg, Germany (K.G.); Division of Tumor Virology (F010), Deutsches Krebsforschungszentrum, Heidelberg, Germany (K.G., I.K., A.A., R.K., L.D., N.T., J.R., J.R.S.); Department of Neurological Surgery, University of Freiburg, Freiburg, Germany (M.H.C.); Department of Neuropathology, University of Mainz, Mainz, Germany (C.S.); Cancer Virotherapy Unit (U 701), Institut National de la Santé et de la Recherche Médicale (INSERM), Heidelberg, University of Heidelberg, Germany (I.K., L.D., J.R.); Department of Radiology, The Ohio State University, Columbus, Ohio (R.K.)*

Oncolytic virotherapy is a potential treatment modality under investigation for various malignancies including malignant brain tumors. Unlike some other natural or modified viruses that show oncolytic activity against cerebral neoplasms, the rodent parvovirus H-1 (H-1PV) is completely apathogenic in humans. H-1PV efficiently kills a number of tumor cells without harm to corresponding normal ones. In this study, the concept of H-1PV-based virotherapy of glioma was tested for rat (RG-2 cell-derived) and for human (U87 cell-derived) gliomas in immunocompetent and immunodeficient rat models, respectively. Large orthotopic rat and human glioma cell-derived tumors were treated with either single stereotactic intratumoral or multiple intravenous (iv) H-1PV injections. Oncolysis was monitored by magnetic resonance imaging and proven by histology. Virus distribution and replication were determined in brain and organs. In immunocompetent rats bearing RG-2-derived tumors, a single stereotactic intratumoral injection of H-1PV and multiple systemic (iv) applications of the virus were sufficient for remission of advanced and even symptomatic intracranial gliomas without damaging normal brain tissue or other organs. H-1PV therapy resulted in significantly improved survival (Kaplan–Meier analysis) in both the rat and human

glioma models. Virus replication in tumors indicated a contribution of secondary infection by progeny virus to the efficiency of oncolysis. Virus replication was restricted to tumors, although H-1PV DNA could be detected transiently in adjacent or remote normal brain tissue and in noncerebral tissues. The results presented here and the innocuousness of H-1PV for humans argue for the use of H-1PV as a powerful means to perform oncolytic therapy of malignant gliomas.

**Keywords:** cathepsin, glioma, oncolytic virus, parvovirus H-1, virotherapy.

**M**alignant brain tumors of glial origin are almost always fatal, and only 50% of patients survive the first year after the diagnosis has been established. Recent modifications of standard treatments, including tumor removal, radiation therapy, and chemotherapy, have only led to a modest improvement in the outcome of the disease.<sup>1,2</sup> Therefore, oncolytic viruses have been investigated, among others, as a novel and promising treatment modality for malignant brain tumors. The panel of candidate viruses includes genetically modified viruses, such as herpesvirus, poliovirus, or adenoviruses, and wild-type viruses, such as reovirus, myxoma virus, vaccinia virus, vesicular stomatitis virus (VSV), or Newcastle disease virus.<sup>3,4</sup> In addition to intratumoral application, systemic therapy was shown to impair glioma growth using VSV.<sup>5,6</sup>

Another promising candidate virus, the rodent parvovirus H-1 (H-1PV), exerts cytotoxic effects that are targeted at a number of neoplastic (including glioma) cells

Received March 8, 2009; accepted January 25, 2010.

Corresponding Author: Karsten Geletneky, MD, Department of Neurological Surgery, University of Heidelberg, Im Neuenheimer Feld 400, 69120 Heidelberg, Germany (K.Geletneky@Dkfz-Heidelberg.de).

<sup>†</sup>These authors contributed equally to this study.

while being innocuous for normal (nontransformed) corresponding cells.<sup>7,8</sup> Though the virus can enter most nontransformed (normal) cells, infection is abortive and fails to produce progeny virions.<sup>9</sup> In contrast, in many malignant cells or in cells transformed by various means, H-1PV infection leads to cell killing, which is not observed in the corresponding nontransformed cells, and can be productive.<sup>10,11</sup> The enhanced permissiveness of transformed cells for H-1PV was shown to be due at least in part to changes in factors associated with (i) cell cycling and differentiation<sup>8,9,12</sup> and (ii) controlling viral DNA replication and gene expression. H-1PV is able to kill malignant brain tumor cells that are resistant to apoptosis-inducing agents like TRAIL or chemotherapeutics. This killing effect on human glioma cells was attributed to the initiation of autophagy followed by the relocation and activation of intracellular cathepsins.<sup>13</sup> H-1PV is able to induce viremia after experimental infection of humans, yet there is no evidence for an association between any human disease and a previous infection with H-1PV.<sup>7,14,15</sup> Previously, we reported the high susceptibility of human and rat glioma cells in culture to the cytotoxic effects of wild-type H-1PV.<sup>16</sup> In order to evaluate the anticancer potency of H-1PV *in vivo*, we analyzed in the present work the oncosuppressive effect of this virus in orthotopic rat models of malignant glioma derived from implanted rat RG-2 cells<sup>17</sup> or human U87 cells. The response of brain tumors was monitored by magnetic resonance imaging (MRI). On the basis of initial findings that H-1PV is able to cross the blood–brain barrier in healthy animals, we used both local and systemic routes of virus application. The data show that injection of H-1PV through either route can induce regression of gliomas without adverse side effects. This proof of concept study makes H-1PV a promising candidate for oncolytic virotherapy of gliomas, particularly as previous studies show no pathogenicity of this virus in humans.<sup>14</sup>

## Materials and Methods

### Cells

The rat glioblastoma cell line RG-2 (kindly provided by C. Walz, University of Magdeburg, Germany) and cells of the human glioblastoma line U87 (obtained from the DKFZ Tumorbank) were grown in DMEM (Sigma-Aldrich) supplemented with 10% FCS (Biochrom KG) and 1% antibiotics (penicillin, streptomycin; Gibco, Invitrogen Corporation) in a 5% CO<sub>2</sub> humidified atmosphere at 37°C. Exponentially growing cells to be injected in rat brains were trypsinized and centrifuged (146 g/10 min), and the pellet was resuspended in DMEM without supplements.

### H-1PV Production and Infection

H-1PV was amplified in human NBK cells and purified on iodexanol gradients as described previously.<sup>13</sup>

H-1PV was titrated on NBK indicator cells by plaque assay and further used at multiplicities of infections expressed in plaque-forming units (pfu) per cell.

### Animal Experiments

All animal experiments were carried out in accordance with institutional and state guidelines.

### Intracerebral Implantation of Tumor Cells

**RG-2 model.** Female Wistar inbred rats (Charles River) were anesthetized with Isoflurane (2.5% and 1.6% as initial and maintenance doses, respectively) and mounted to a stereotactic frame. After linear scalp incision, a 0.5-mm burr hole was made 2 mm right of the midline and 1 mm anterior to the coronal suture. The needle of a 10- $\mu$ L Hamilton syringe was stereotactically introduced through the burr hole into the frontal lobe at a depth of 5 mm below the level of the dura mater, and RG-2 glioma cells (3000 cells in a volume of 3  $\mu$ L) were injected over 3 minutes. The needle was withdrawn slowly to minimize spreading of tumor cells along the needle tract.

**U87 (a human glioma cell line) model.** Immunodeficient RNU rats (Charles River) were anesthetized as described above and placed in a stereotactic frame. A burr hole was made at the same coordinates and  $1 \times 10^5$  U87 cells in a volume of 5  $\mu$ L were injected 5 mm below the level of the dura mater over 5 minutes. The needle was left in place for 2 minutes and withdrawn at a speed of 1 mm/min.

### Intracranial Stereotactic Infection of RG-2 Gliomas with H-1PV

Animals harboring large gliomas exceeding 170 mm<sup>3</sup> in size (determined by MRI analysis, see below) were infected with H-1PV by stereotactic injection of the virus into the tumor. After guiding the injection cannula to the same coordinates, the H-1PV inoculum (14  $\mu$ L;  $1.4 \times 10^7$  pfu) was applied in fractions of 2  $\mu$ L to different locations within the tumor by gradually reducing the depth of injection from the most basal tumor margin visualized by MRI.

### Intravenous Infection of RG-2 Glioma-Bearing Animals with H-1PV

After confirmation of intracerebral tumor growth (size: >100 mm<sup>3</sup>) by MRI, animals were injected with H-1PV in the tail vein. The volume of injection was 100  $\mu$ L (corresponding to a dose of  $1 \times 10^8$  pfu) on day 1 of treatment, and 50  $\mu$ L ( $5 \times 10^7$  pfu) on the following days. Animals were treated with 8 or 12 injections on days 1–8 or days 1–12, respectively. MRI was performed to monitor the therapeutic effect.

### *Infection of U87 Glioma-Bearing Animals with H-1PV*

RNU rats with U87 xenografts were treated with H-1PV through multiple injections. The first application used both the intracranial (ic) (10  $\mu$ L) and intravenous (iv) (190  $\mu$ L) routes, and for subsequent applications (at 4-day intervals) the iv route only (100  $\mu$ L). The total dose of H-1PV per animal was  $6 \times 10^9$  pfu. In one group of animals, the treatment was initiated when gliomas were small, but clearly visible (“early” infection). In a second group, animals with larger tumors were treated with H-1PV at a later time point (“late” infection). The control group consisted of mock-treated animals with tumors of respective sizes, and animals were randomly assigned to receive virus or mock treatment.

### *Magnetic Resonance Imaging*

The animals were examined in a 2.45-T MRI scanner (Bruker) using T1-weighted imaging before and after injection of 0.4 mL contrast medium (Gadodiamide, Omniscan, Amersham) into the tail vein. Gadodiamide-enhanced T1 imaging was performed 5 minutes after injection. During MR examination, rats were anesthetized by isoflurane insufflation (initial dose 2.5%, maintenance 1.6%). Tumor volumes were determined using MRIcro software (www.mricro.com).<sup>18</sup>

### *Statistics*

Survival times of treated and control animals were statistically analyzed using methods for censored failure times for carcinogenicity experiments.<sup>19</sup> The survival curves were described by the Kaplan–Meier method, and the time course of the number of animals at risk was reported there as well. Prior to starting the experiments, it was planned to serially sacrifice animals from the experimental group, based on MRI, in order to get additional pathological information. Survival times of treated animals sacrificed for analysis were therefore censored at the date of sacrifice. For comparing the survival times in the H1PV treated (ic or iv) versus the control animals, we used the log rank test for censored survival times. Statistical significance was reported as *P* value and stated as significant if *P* < .05.

### *Tissue Preparation*

Animals were killed with CO<sub>2</sub> at different times after injection of H-1PV. Organs were removed and either fixed in formalin and embedded in paraffin for histological analysis, or frozen at  $-192^\circ\text{C}$  (liquid nitrogen) after immersion in freezing medium for cryosections (TissueFreezing Medium, Jung) or as tissue samples.

### *DNA and RNA Extraction from Tissue Samples*

Specimens from brain (normal tissue and tumor) and from various organs (heart, lung, liver, spleen, and kidney) were shock-frozen in liquid nitrogen. Isolation

of DNA was done using the High-pure PCR Template Preparation Kit (Roche Diagnostics GmbH). The extracted DNA was either used immediately for PCR analysis or stored at  $-20^\circ\text{C}$ .

RNA was isolated using the High-pure RNA Tissue Kit (Roche Diagnostics GmbH). Eluted RNA was analyzed immediately (RT–PCR) or stored at  $-80^\circ\text{C}$  for further analysis.

### *PCR Analyses*

For PCR analysis of H-1PV DNA, Supermix (Invitrogen) was used. PCR was performed with the following primers: sense primer, 5'-TCAATGCGCTCACCATC TCTG-3' (position nt 1996–2016 within the NS gene region of the H-1PV genome) and antisense primer 5'-TCGTAGGCTTCGTCGTGTTCT-3' (position nt 2490–2510). DNA from the H-1PV plasmid CIII $\Delta$ 800 (courtesy of C. Dinsart<sup>20</sup>) served as a positive control.

For RT–PCR detection of H-1PV transcripts (NS gene), the same primers were used. As these primers anneal to exon sequences flanking a small intron, 2 different products were amplified whenever contaminating DNA was present in the RNA sample: the product amplified from cDNA deriving from the reverse transcribed intronless mRNA and a slightly larger product generated from (contaminating) DNA.

### *Immunohistochemistry*

For immunostaining of the parvoviral NS-1 protein, deparaffinated and appropriately blocked 12  $\mu$ m sections mounted on slides were incubated for 12 hours with the monoclonal NS-1-specific antibody 3d9 (courtesy of N. Salomé) and an Alexa Fluor-conjugated donkey anti-mouse secondary antibody (Invitrogen), and were counterstained with DAPI (Sigma). For cathepsin B immunostaining, the specific clone CB 59-4B11 (courtesy of E. Weber, Halle, Germany) and an anti-rabbit Cy3-conjugated antibody (Santa Cruz) were used as primary and secondary antibodies, respectively. Slides were analyzed with a DM-RBE automated fluorescence microscope (Leica), and images were processed using the Openlab software (Improvision).

### *Detection of Progeny Virus in Brain Tissue*

Tumor bearing and control (glioma-free) animals were injected intracranially with H-1PV as described above. Two days post-infection (p.i.), the animals were sacrificed, brains were removed surgically, and equal volumes of brain samples were homogenized in 2 mL PBS per brain sample, in the presence of Matrix-D beads (Q-Biogene,  $2 \times 40$  seconds, speed 4). Four milliliters of washing solution (PBS) were added, followed by centrifugation for 10 minutes at 1310 g. This supernatant was filtered through 0.45  $\mu$ m filters and used in serial dilutions (1:10 steps) for infection of RG-2 indicator cells.

### Quantification of Neutralizing Antibodies

Blood samples were obtained from Wistar rats at different time points after H-1 virus infection. Whole blood was centrifuged (582 g/10 min) and the serum was diluted in serum-free MEM ( $10^{-1}$  to  $10^{-8}$ ). Each dilution was mixed with H-1PV ( $8 \times 10^4$  pfu in a volume of 20  $\mu$ L) and incubated for 30 minutes at room temperature. Semiconfluent NBK cells in 96-well dishes ( $8 \times 10^3$  cells/well) were incubated with the serum/virus mixture for 20 minutes. Then, medium (MEM containing 5% heat-inactivated FCS and 1% penicillin-streptomycin) was added to the wells, the cells were incubated for 72 hours at 37°C, and inhibition of viral CPE was analyzed by measuring cell viability (MTT test). The virus-neutralizing antibody titer was defined as the dilution of serum that protected 50% of the NBK cells from the virus-induced cytopathic effects.<sup>21</sup>

### Cell Proliferation Assay (MTT Test)

Proliferation of indicator cells was measured using the MTT test. In brief, MTT (3-[4,5 dimethylthiazol-2-yl]-2,5-diphenyltetrazolium bromide, Sigma-Aldrich) stock solution (5 mg/mL) was added at a 1:10 dilution to each well containing NBK cells, and cultures were incubated for 3.5 hours at 37°C. The medium was removed and the converted dye was solubilized with acidic isopropanol (100  $\mu$ L). Extinction values were measured with a Multiskan EX (Thermo Electron Corporation) at 570 nm.

## Results

### Oncolytic Virotherapy of RG-2 Gliomas by Intratumoral Injection of H-1PV

To analyze the oncosuppressive effect of H-1PV, we first used an established immunocompetent rat model of advanced malignant glioma growing from stereotactic ic implantation of rat RG-2 cells.<sup>17</sup> Tumor growth was monitored by MRI, revealing the development of a contrast medium enhancing intracerebral mass detectable when the tumor volume reached 30 mm<sup>3</sup>. Animals harboring gliomas larger than 170 mm<sup>3</sup> in size were infected with H-1PV by stereotactic injection of virus into the tumor. As the rate of tumor growth varied between individual animals, the time of H-1PV treatment was based on tumor size (measured by MRI<sup>18</sup>) and not on days after tumor cell implantation (average time after tumor cell implantation: 16.5 days; average tumor size: 268 mm<sup>3</sup>). In these experiments, different virus preparations were used and standardized to the same titer prior to injection. In previous experiments, stereotactic injection of this virus dose into the brain of nontumor bearing animals did not induce any pathological alterations (data not shown).

Using this individualized approach, 12 tumor-bearing animals were treated with stereotactic injection of H-1PV in the tumor, and tumor growth was compared

with untreated controls ( $n = 12$ ). The experiments were carried out in groups of 4 animals each. The experimental setup allowed for follow-up MRI examinations and individualized timing of H-1PV treatment based on MRI findings for each animal. All control animals had to be sacrificed between days 14 and 22 after tumor implantation, when tumor volumes exceeded 450 mm<sup>3</sup> and animals showed symptoms of raised ic pressure.

Among the H-1PV-treated animals, 8 of 12 rats responded with a progressive reduction in tumor size and changes in tumor morphology on MRI as early as 3 days after treatment. As shown in Figs. 1 (A2) and 3 (C and I), the intensity of contrast enhancement in virus-injected central areas of the tumors was reduced. The animals in Fig. 3 were sacrificed (6 days p.i., animal #74 and 3 days p.i., animal #61) to make tissue sections available for histological analysis. As shown in Fig. 3 (D, E, J, and K), the area of reduced contrast enhancement corresponded to large necrotic areas in the tissue (H&E staining). Four of the 8 responding animals had complete tumor remission (exemplified for animal #100 in Fig. 1) and have survived for more than 1 year, without any remaining or recurrent tumor tissue. The other 4 of the responding 8 animals were sacrificed for further analysis at a stage of tumor regression ranging from 30% to 70% compared with maximum tumor volume on MRI. All of these animals were without clinical symptoms at the time (see Fig. 3 showing animals #74 and #61 with different degrees of antitumor response). When present at the time of virus injection, tumor-associated clinical symptoms (apathy, absent grooming, reduced arousal, and loss of body weight) resolved in the case of successful viral therapy. Four of the 12 treated rats showed continuous tumor growth on follow-up MRI and had to be sacrificed between days 17 and 24 after tumor cell implantation, like control animals. However, also in these animals, the injected tumors showed areas of clear oncolytic effects similar to the changes in regressing tumors (Fig. 3J and K).

Statistical comparison revealed that injection of H-1PV into advanced RG-2 gliomas resulted in significantly longer survival compared with control animals ( $P < .001$ ; Fig. 2) for ic treatment as well as for iv treatment.

Histological analyses showed extensive destruction of the tumor without any pathological alteration of the surrounding normal brain tissue and only minor signs of inflammation (Fig. 3). Paralleling our recent results on the role of activation of cathepsin B in the oncolytic effect of H-1PV *in vitro*,<sup>13</sup> sections of injected tissues showed activation of cathepsin B expression only in H-1PV-infected tumor cells (Fig. 4, Panel 4), indicating a nonapoptotic death process. As shown in Fig. 4A, parvoviral DNA could be detected in the tumor tissue and in peritumoral brain tissue 48 hours p.i. The spreading of the virus appeared to increase after 72 hours when viral DNA could additionally be detected in the contralateral brain hemisphere, in the cerebellum, and in distant organs (heart, lung, liver, spleen, and kidney), yet only



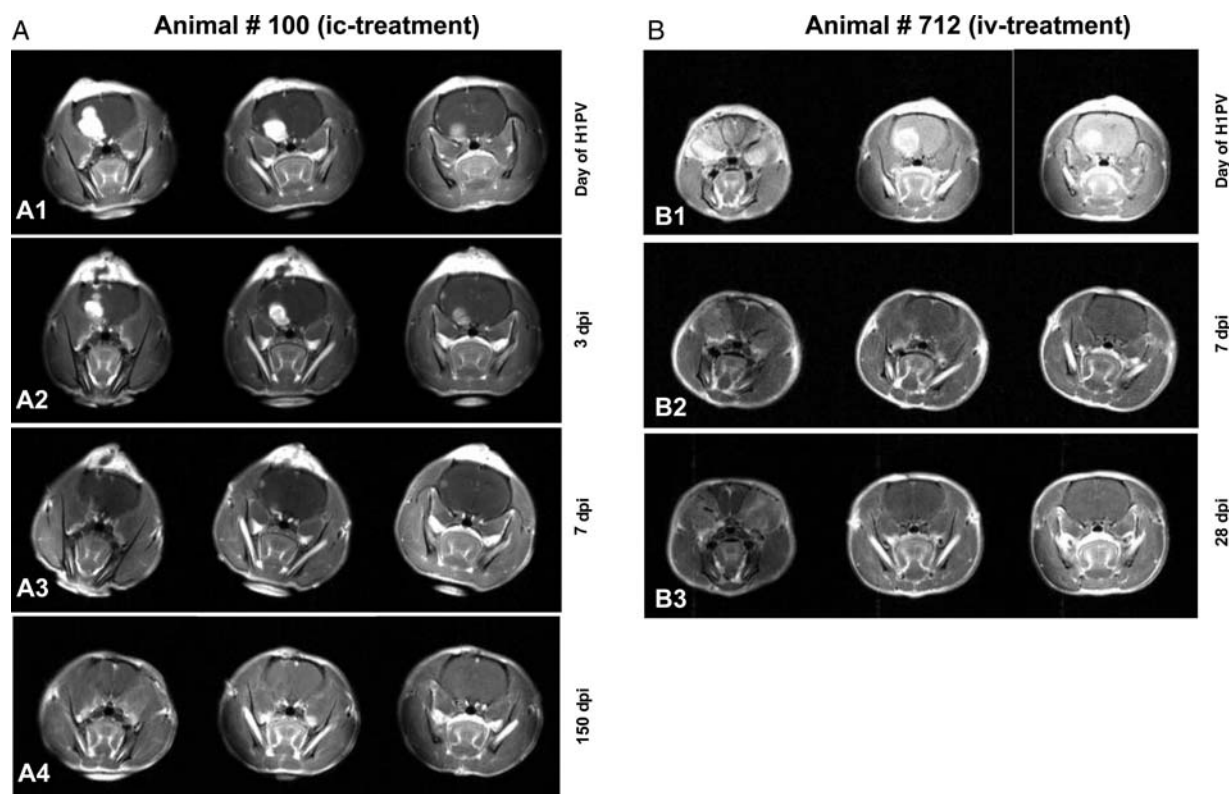


Fig. 1. Complete remission of RG-2 gliomas after H-1PV treatment MR images of animal #100 (A1 to A4) and #712 (B1 to B3) at different time points. For each examination, 3 coronal sections are shown. Tumor volumes defined by the area of contrast enhancement progressively decreased after H-1PV injection. Animal #100 was infected with H-1PV intratumorally (A1) and examined on days 3, 7, and 150 p.i. (A2, A3, and A4, respectively). Examination dates for animal #712, which was infected intravenously (B1), were days 7 and 28 p.i. (B2 and B3). Both animals have survived for more than 6 months and without tumor recurrence.

transiently since no viral DNA could be revealed in any tissue 2 weeks p.i. (Table 1). Viral transcripts and proteins could be detected in (residual) tumor tissue by RT-PCR and immunohistochemical analyses (presence of the viral NS protein), respectively. However, parvovirus transcription and accumulation of the replicative cytotoxic nonstructural viral protein NS-1 were restricted to the tumor remnants and undetectable in surrounding normal tissues (Fig. 4, Panel 2), arguing for the selective replication of the virus in tumor cells. This was confirmed by testing virus multiplication after injection of H-1PV in tumor bearing and control rat brains. The yield of infectious virus isolated from the brain 2 days after H-1PV injection was 2 orders of magnitude higher in extracts from H-1PV-treated tumor-bearing animals compared with brain extracts from control animals lacking tumor cells, injected with the same amount of virus (data not shown). Obviously, tumor tissue supported virus replication and the release of progeny virus, resulting in viremia and uptake of progeny particles at extratumoral sites, yet without further virus replication at these sites.

#### *Oncolytic Virotherapy of RG-2 Gliomas by iv Injection of H-1PV*

On the basis of the finding that H-1PV was able to permeate the blood–brain barrier, 9 animals with

RG-2 gliomas exceeding  $100 \text{ mm}^3$  in size received iv injections of the virus to assess whether sufficient amounts of virus particles could also be delivered to the tumor via this route of administration. Animals were treated with 8 or 12 injections on 8–12 consecutive days ( $1 \times 10^8$  pfu on day 1;  $5 \times 10^7$  pfu on the following days). It is noteworthy that H-1PV-neutralizing serum antibodies appeared 5–7 days after iv (or ic) injection of the virus (data not shown). In 6 of 9 treated animals, tumors regressed completely even when the treatment was reduced from 12 to 8 injections. MRI analyses between 2 and 3 weeks after initiation of treatment showed no remaining tumor tissue in these animals. None of these animals have developed recurrent tumor growth during an observation period of 6 months after the treatment. Like intratumoral treatment, iv injection of H-1PV significantly improved survival of glioma-bearing animals ( $P < .001$ ; Fig. 2) and did not induce any side effects in other organs. Three days after iv infection, viral NS-1 protein expression was only observed in tumor tissue but not in adjacent brain cells (Fig. 4). As in the case of intracerebral injection of H-1PV, iv application resulted in detection of viral DNA in the tumor and various organs, including the contralateral hemisphere of the brain, spleen, liver, and lung (M. Friedel, unpublished thesis). Viral DNA first appeared in brain, liver, and spleen, and gradually

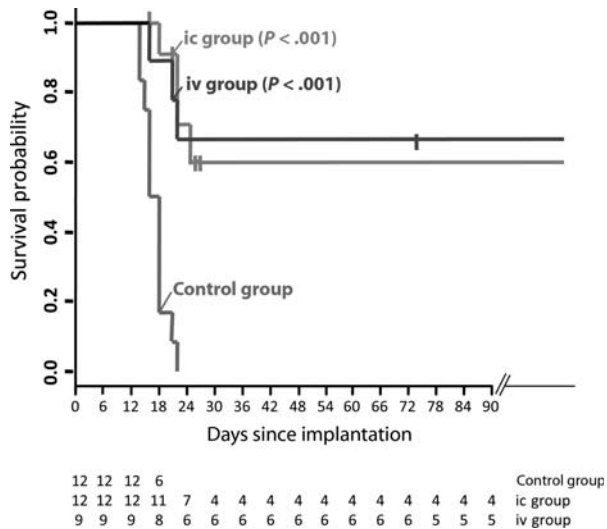


Fig. 2. Prolonged survival following intratumoral or iv H-1PV treatment of RG-2 gliomas. The survival of H-1PV-treated (ic and iv) and control animals is presented using the Kaplan–Meier method. Survival times of treated animals sacrificed for analysis were censored at the date of sacrifice, marked by vertical bars. Values below the plot give the numbers of animals at risk, equivalent to surviving animals on the respective days. The difference between the treated groups and the controls was statistically significant (log rank test:  $P < .001$ ) both for ic and iv. See also the “Materials and Methods” section.

declined starting from approximately 1 week p.i. and eventually disappeared from all tissues. Altogether, these data demonstrate that iv-administered H-1PV is able to cross the blood–brain barrier, reach gliomas, and become amplified in these tumors.

#### Oncolytic H-1PV Therapy of U87 Glioma Xenografts

In order to test the activity of H-1PV in human gliomas, we established tumors derived from the human U87 glioma cell line in immunodeficient rats (RNU). H-1PV treatment was administered by combined ic and iv virus injection either at an early time point of tumor development (small tumors, 6 animals) or at a later stage (larger tumors, 6 animals), on the basis of MRI (designated in Fig. 5 as “early” and “late” infection, respectively). In order to substantiate viral oncolytic effects detected by MRI, treated animals were sacrificed at different time points (28, 41, 42, or 60 days after tumor cell implantation). At the time of killing, no pathological signs were detectable in infected animals, which appeared healthy, were active, and continued to gain body weight. This contrasted with uninfected control animals, which survived 21 days maximum after tumor cell implantation. In the “early infection” group, H&E staining of brain cryosections from H-1PV-treated animals showed evidence of tumor destruction on day 28 after tumor cell implantation and complete elimination of tumor tissue from day 42 on (data not shown), confirming radiological findings

by MRI. In the “late infection” group, tumor regression was not complete (Fig. 5), yet tumor growth fully stopped, and all animals survived until they were sacrificed for analytical purposes. Both early and late H-1PV treatments resulted in a significantly prolonged survival of animals with human glioma xenografts. In infected rats, expression of the cytotoxic parvoviral NS-1 protein could be detected by immunofluorescence (Fig. 5) in necrotic tumor areas but not in the surrounding normal brain tissue, confirming above observations in immunocompetent animals.

## Discussion

The goal of this study was to determine the oncolytic efficiency of H-1PV against intracerebral gliomas in animal models. The data show the capacity of H-1PV to eliminate even advanced and symptomatic glioma xenografts in the absence of pathogenic effects on normal tissues, including adjacent brain areas. This is in line with the innocuousness of H-1PV for adult rats in natural infections.<sup>22</sup> In most studies of virus-based local therapy of ic gliomas, the treatment was initiated within only a few days after tumor cell implantation.<sup>23–27</sup> Recently, a prolonged survival of symptomatic animals after viral therapy with an oncolytic herpesvirus was reported.<sup>28</sup> Although in this setting the virus (HSV-1) was able to cure animals when administered 14 days after tumor implantation, it prolonged survival, but failed to eradicate the tumor in cases of advanced and symptomatic disease after 19 days. Also in the models used for iv treatment of gliomas with VSV, the lethal effect of the virus prevented assessment of long-term survival. As shown here for oncolytic parvo-(H-1PV)virotherapy, a complete cure of animals symptomatic from gliomas at late tumor stages could be achieved, resulting in long-term survival.

The efficiency of H-1PV in inducing glioma regression is likely to be boosted by an increase in the initial virus dose as a result of the replication of input virus in primarily infected tumor cells, followed by spreading of progeny virus to and secondary infection of remaining tumor cells. In keeping with this mechanism, H-1PV DNA, transcripts, and proteins (in particular the nonstructural viral products driving replication) accumulated in the tumor (remnants), starting from a few days after virus injection. Furthermore, indication of transient viremia originating from the tumor was given by the time-dependent transfer of viral DNA to nontumoral tissues, first in the periphery of the lesion and subsequently in distant organs. Infection of nontumoral tissues appeared to be cryptic as no H-1PV gene expression could be detected even when these tissues tested positive for the presence of viral DNA, which vanished within 2 weeks p.i. This specificity of H-1PV replication and cytopathogenicity for neoplastic tissues, in particular gliomas, shows that the parvovirus keeps under *in vivo* conditions the oncotropism that it displays in cell cultures.<sup>13,16</sup> The spreading of the virus through the brain and to other organs could be of therapeutic

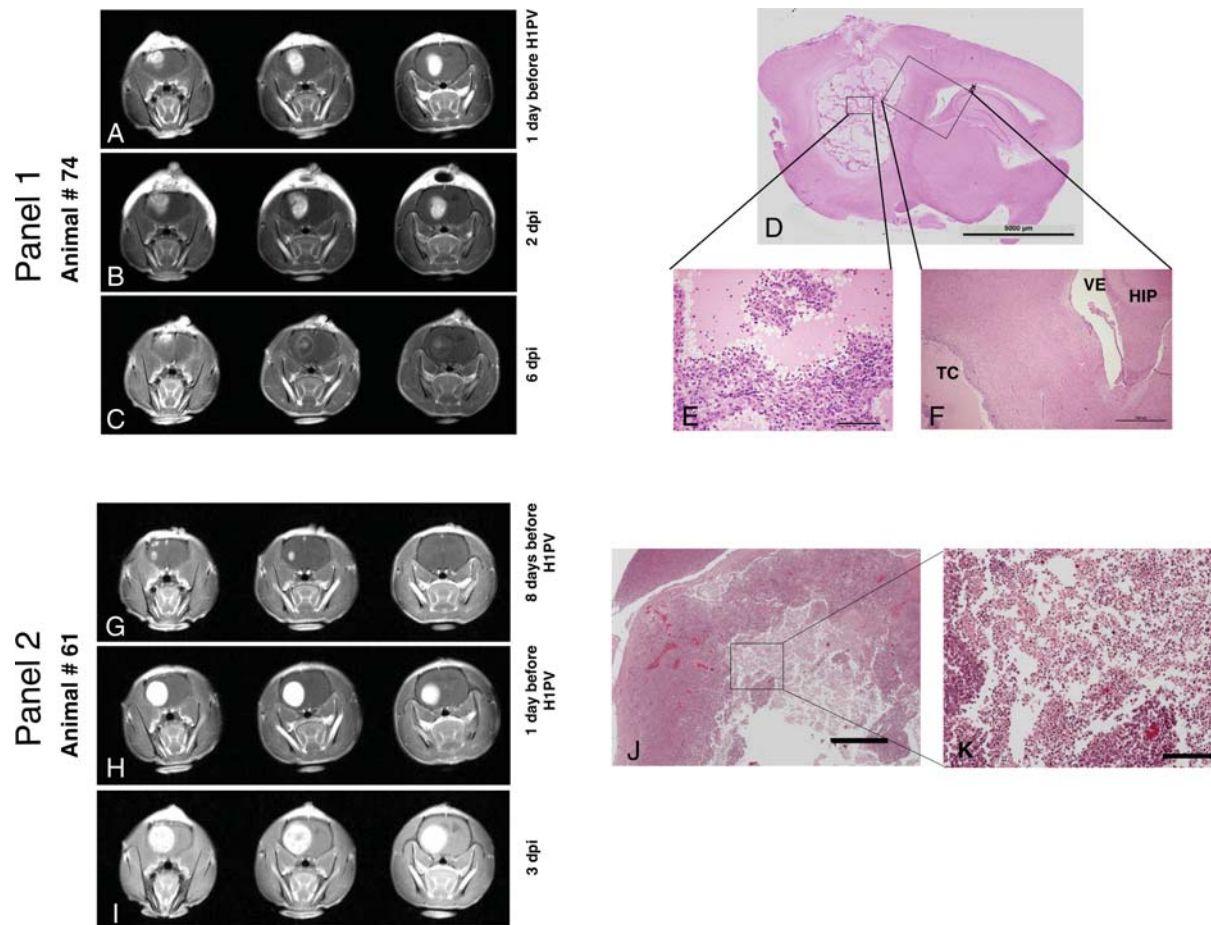


Fig. 3. Analyses of oncolytic effects in gliomas after H-1PV infection. Panel 1: Regressing tumor (A–C): Tumor regression by MRI (different time points relative to H-1PV infection, 3 coronary sections shown for each examination date). (A) One day before H-1PV administration (15 days after tumor cell implantation), a large tumor was visible in the right frontal lobe. (B) Two days after stereotactic injection of H-1PV, the area of contrast enhancement had slightly increased in volume but displayed a more inhomogeneous appearance (which was associated with an improvement in clinical symptoms). (C) On day 6 p.i., the tumor showed a massive reduction in contrast uptake and an entirely different staining pattern, with a rim-like appearance and only a few areas of remaining enhancement in the central and the most superficial parts of the tumor. The animal was without any clinical symptoms of cerebral or other origin and was sacrificed on this day for further analysis. (D–F) Histological analysis of the area of H-1PV-induced glioma destruction in above animal. (D) In this sagittal section of the entire right hemisphere of the brain (H&E staining; scale bar 5 mm), a large cavity was visible in the location of the initial tumor, whereas surrounding and distant brain tissue had a normal appearance. (E) At a higher ( $\times 20$ ) magnification, the tumor cavity appeared to be composed of islands of remaining vital tumor cells embedded in an amorphous eosinophilic mass. Scattered granulocytes, erythrocytes, and plasma cells were detectable, in particular at the periphery of the tumor cell islands. (F) A  $\times 4$  magnification of the oblique box in D shows part of the tumor cavity (TC) and adjacent normal structures of the brain such as the ventricle (VE) and the hippocampus (HIP). A few tumor cells were visible underneath the ependyma of the ventricular wall. Scattered lymphocytes and plasma cells were present in the immediate vicinity of the tumor cavity. Otherwise, no significant pathological alterations were detectable within the normal tissue adjacent to the tumor. Panel 2: Progressing tumor in spite of H-1PV therapy (G–I): MR analysis. (G) Eight days before H-1PV administration (10 days after tumor cell implantation), a small tumor began to develop in the right frontal lobe. (H) One day before treatment with H-1PV, the tumor occupied almost the entire right frontal lobe, demonstrating the rapid growth of the glioma. (I) On day 3 p.i., the tumor had further increased in volume. The animal had become symptomatic and was sacrificed on this day. Of note, the uptake of the contrast agent (gadolinium) was less homogeneous in central areas of the tumor injected with H-1PV (I, middle image) compared with the previous time point (H), similar to early changes in regressing tumor (panel 1, B and C). (J and K) Histological analysis. (J) At a low magnification ( $\times 2$ , scale bar 1000  $\mu\text{m}$ ), histological appearance of the tumor (H&E staining) showed pale staining of necrotic tissue in the center. (K) At a higher magnification ( $\times 10$ , scale bar 200  $\mu\text{m}$ ), oncolysis was characterized by numerous cells with shrunken nuclei (similar to image E, panel 1) as well as necrotic/autolytic ghost cells indicating lytic activity of H-1PV.

significance. One main obstacle in the treatment of malignant gliomas lies in the early migration of tumor cells away from the primary tumor site, resulting in

reduced accessibility for local therapies. Secondary rounds of infection by oncolytic viruses without further spreading of progeny particles beyond the



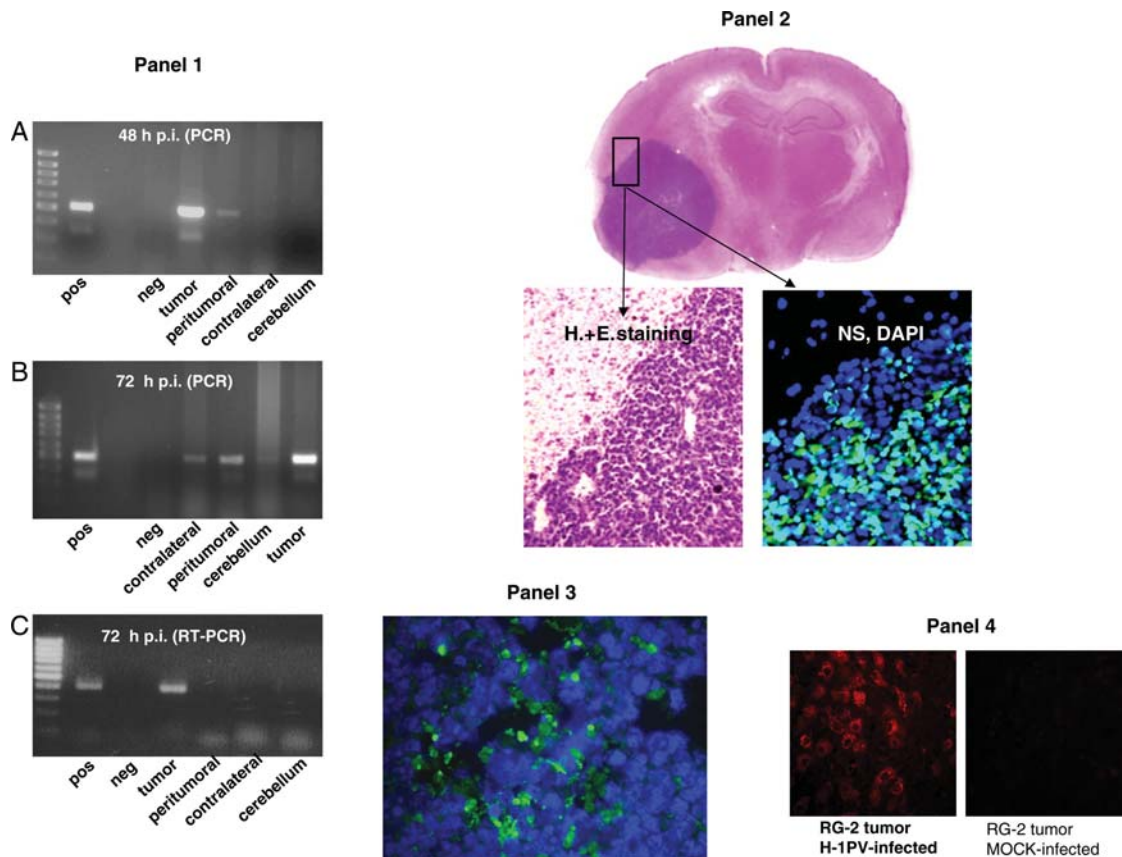


Fig. 4. Distribution of viral and cellular markers in the brain of rats following glioma injection with H-1PV. Panel 1: PCR detection of H-1PV DNA (A and B) and RNA (C). The presence of H-1PV DNA in the treated tumor, adjacent brain tissue (peritumoral), contralateral hemisphere, and cerebellum (as indicated) was determined by PCR 48 hours (A) or 72 hours (B) after intratumoral virus injection. The production of H-1PV transcripts at the same locations was tested by RT-PCR 72 hours after intratumoral injection of H-1PV (C). Amplified fragments were detected after agarose gel electrophoresis. The primers used anneal to exon sequences flanking a small intron, resulting in a slightly larger product amplified from DNA compared with intronless cDNA. pos, positive control (H-1PV plasmid DNA); neg, negative control (double-distilled water); far left lanes, size markers (DNA ladder). Panel 2: Immunohistochemical detection of parvoviral NS-1 proteins. Sections were prepared from RG-2 glioma and adjacent (brain) tissues, collected 2 days after intratumoral injection of  $1.6 \times 10^7$  pfu of H-1PV. The fluorescence signal indicating the presence of NS-1 proteins is restricted to the tumor area and could not be detected in adjacent tissue (DAPI staining of nuclei on the same image). For orientation, H&E staining of the same brain area is shown at low and high magnification. Panel 3: Immunohistochemical detection of parvoviral NS-1 proteins in glioma tissue after iv injection. Sections were prepared 3 days after iv injection of  $10^8$  pfu of H-1PV. The green fluorescence demonstrates the parvoviral NS-1 protein scattered throughout the tumor tissue, proving that iv-administered H-1PV reached the brain tumor and is expressed. Panel 4: Impact of H-1PV infection on cathepsin B expression in RG-2 gliomas. An established RG-2 tumor was injected with H-1PV or mock-treated and removed 72 hours later for sectioning and immunohistochemical detection of cathepsin B. Virus infection correlated with a striking activation of cathepsin B, a known effector of H-1PV-induced glioma cell death. No cathepsin B signal was detected in mock infected tumors.

margins of the tumor might therefore not be sufficient for successful virotherapy.

An additional advantage of H-1PV lies in its ability to circumvent the mechanisms allowing glioma cells to resist other cytotoxic agents. This feature was traced back to the capacity of the parvovirus to activate a non-conventional, cathepsin-mediated death pathway as recently demonstrated in cultures of H-1PV-infected glioma cells.<sup>13</sup> The selective up-regulation of cathepsin B in tumor tissues of animals treated with H-1PV is in line with these *in vitro* findings and is most likely induced by the virus. However, the detailed analysis of

death pathways after H-1PV infection *in vivo* was beyond the scope of this proof of concept study.

The antiglioma effect of H-1PV could be achieved both by direct ic injection of the virus inoculum into the tumor and by repeated iv injection. This study shows for the first time the capacity of H-1PV to cross the blood–brain barrier and target and destroy ic gliomas. To achieve this effect, the virus dose was 50-fold higher than by stereotactic treatment, and even this high concentration of viral particles did not cause any side effects in treated animals. H-1PV infection resulted in oncolytic effects within the tumor in all



**Table 1.** Distribution of H-1PV DNA in the brain and organs at different time points after infection (PCR analysis)

Animal ID*	Days p.i.	Specimen or organ								
		Tumor	Brain peritumoral	Brain contralateral	Cerebellum	Heart	Lung	Liver	Spleen	Kidney
A	2	+	+	neg	neg	+	+	+	+	+
B	3	+	+	+	+	+	+	+	+	+
C	3	+	+	+	+	+	+	+	+	+
D	4	+	+	+	+	+	+	+	+	+
E	8	+	+	+	neg	neg	+	+	+	+
F	10	+	+	+	neg	neg	neg	+	+	neg
G	11	+	+	neg	neg	neg	neg	+	neg	+
H	14	neg	neg	neg	neg	neg	neg	neg	neg	neg

\*A separate group of 8 tumor-bearing animals was analyzed for the presence of H1PV DNA (+), at various time points after intratumoral injection of H-1PV (p.i.). "neg", no viral DNA detectable.

animals with progressing gliomas. As obviously not all animals could be cured with either local or systemic therapy, the current methodology may be further improved, for example, by administering the virus through intratumoral convection-enhanced delivery, by further increasing the virus dose, or by combining intratumoral and systemic virotherapy. This possibility for the combination of local and systemic H-1PV application could be a major advantage for future therapy.

The RG-2 model system used in this study allowed viral therapy to be assessed in immunocompetent animals, mimicking in this regard the patient's situation. This setup raises the question of the possible involvement of the immune system in the tumor suppression observed. In our study, implantation of only 3000 RG-2 glioma cells led to the development of a lethal brain tumor in all untreated animals and even in some of the rats that received H-1PV therapy. This is in contrast to Mariani et al.<sup>29</sup> who showed spontaneous regression of RG-2 tumors in this system, correlating with the occurrence of antitumor immune responses. Under our experimental conditions, glioma suppression proved to fully depend on H-1PV infection and to be associated with the expression of viral cytotoxic proteins in regressing tumor areas. Infection of large tumors with subsequent virus production and spreading within the brain and to other organs did not lead to inflammatory changes or related pathology. No obvious infiltration of treated tumors with immune cells was noticed in histological sections. In particular, the number of CD3-positive cells in the tumor area (cryosections) of glioma-bearing rats did not differ significantly between H-1PV and mock-treated animals (11 days post-tumor cell implantation, 4 days p.i.; data not shown). The possibility still needs to be considered that oncolytic H-1PV serves, at least in part, as an adjuvant to promote anticancer vaccination through the release of tumor-associated antigens and additional immunostimulating activities.<sup>30</sup> In keeping with this possibility, a tumor challenge of all 4 cured animals 1 year after successful treatment failed to result in the development of RG-2 gliomas even when cells were injected in 30-fold greater numbers into the contralateral hemisphere

(data not shown). Investigations addressing this observation are currently in progress to assess the capacity of the immune system to take over from the initial oncolytic activity of H-1PV and complete tumor eradication. It should, however, be stated that H-1PV treatment leads to oncolysis and prolonged survival without side effects in immunodeficient animals bearing human glioma xenografts, pointing to the fact that an adaptive cell-mediated immune response is not an absolute prerequisite for H-1PV-induced glioma suppression.

In conclusion, this study produces proof of the concept that H-1PV can be used as an efficient and safe oncolytic virus for glioma treatment in humans using different routes of infection. Although this study was not designed to determine the minimum efficient dose of the virus, it can serve as a basis to calculate the dose range to be administered to humans, by considering a rat to human body weight ratio of 1:300. The titers calculated in this way can be achieved using the H-1PV production system presently available. It should also be noted that, in a previous trial, the inoculation of cancer patients with H-1PV was found to be devoid of significant harmful side effects.<sup>14</sup> In this pilot study, purified virus was injected in accessible skin metastases from different kinds of primary solid tumors. Each patient received 2 or 3 injections of H-1PV, at intervals of 10 days. Single doses administered ranged from  $10^8$  to  $10^{10}$  pfu. Toxicity was absent or mild, and a maximal tolerated dose was not reached. The presence of H-1PV could be demonstrated by a transient viremia and seroconversion as well as by in situ virus replication in neoplastic lesions. This innocuousness of H-1PV to humans, together with the fact that preexisting antiviral immunity (a possible reason for a low efficiency of virus-based treatments) is rare or even nonexistent in the case of H-1PV in the human population,<sup>7</sup> render this parvovirus a very promising candidate for virotherapy.

Altogether, the data presented and discussed in this study lay the foundation for the initiation of a phase I/IIa clinical trial using H-1PV as a novel therapeutic agent for the treatment of patients with high-grade gliomas.

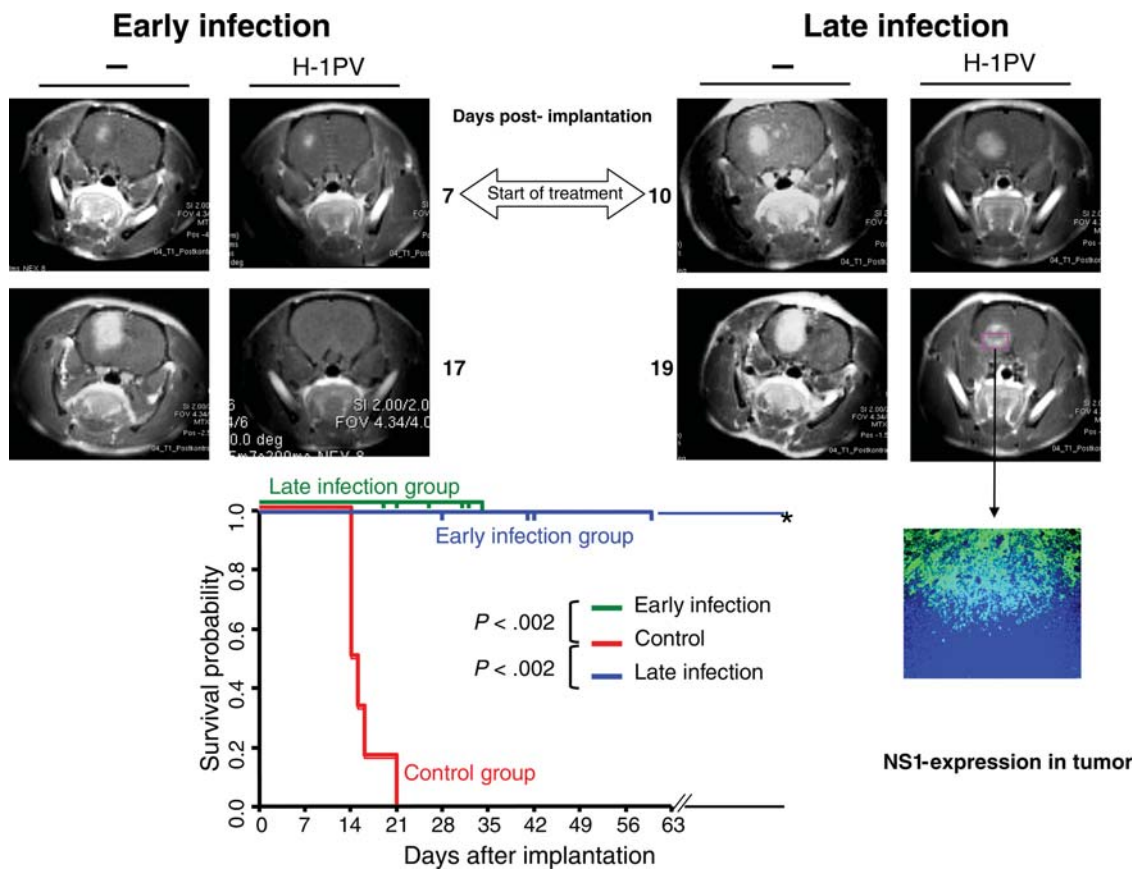


Fig. 5. H-1PV-induced suppression of human gliomas (established from U87 cells) in RNU rats. (Upper panel) Demonstration of tumor regression by MRI (4 representative rat brains; images at different time points relative to tumor cell implantation [ $10^5$  U87 cells per animal], as indicated). (Left MRI) At day 7 after tumor cell implantation, a small tumor was visible in the right frontal lobe of the 2 brains shown. “Early infection” (combined ic and iv infection with H-1PV) was performed at this day. After 10 days (day 17 post-implantation), this tumor had disappeared in the treated animal (“H-1PV”), whereas in the control animal (–) the tumor area had largely increased. (Right MRI) At day 10 after implantation of U87 cells, a relatively large tumor was identified by MRI in both animals’ brains. At this day, “late infection” was performed as described above for “early infection”. In the treated animal, the tumor stopped growing after ic + iv treatment with H-1PV as demonstrated 9 days p.i. (day 19 post-implantation), in contrast to the continuing development of the tumor in the untreated animal (–). Immunohistological examination of the growth-arrested tumor (cryosection of the treated animal’s brain) showed expression of the parvoviral NS-1 protein in the necrotic tumor area. (Lower panel) Significantly improved survival of H-1PV-treated animals compared with controls. Early and late infections refer to the time of virus administration relative to tumor development, corresponding to the treatment of small and large tumors, respectively (see main text). All untreated animals had to be sacrificed because of tumor progression, at the latest on day 21 after tumor cell implantation. All treated animals were killed at various times p.i. for analyses of tumors size and histology. All but one of the treated animals, killed on day 19, survived longer than the controls and were sacrificed for analyses on days indicated separately for early and late infection by vertical bars on the two 100% survival probability lines (horizontal lines at 1.0) representing the survival of the 2 treatment groups. One animal (\*) survived for more than 8 months.

## Acknowledgments

We gratefully acknowledge the skillful and devoted technical assistance of Ms R. Ly. We thank Ms B. Leuchs for preparing virus stocks and Ms M. Krämer for help with immunostaining. We are indebted to Prof. S. Heiland for assistance with MRI, and A. Benner and L. Edler for performing statistical analysis. We thank the personnel of the animal facility of the DKFZ for most valuable support for animal experiments.

*Conflict of interest statement.* None declared.

## Funding

This work was financed in part by grant F203497, University of Heidelberg.

## References

- Stummer W, Pichlmeier U, Meinel T, Wiestler OD, Zanella F, Reulen HJ. Fluorescence-guided surgery with 5-aminolevulinic acid for resection of malignant glioma: a randomised controlled multicentre phase III trial. *Lancet Oncol*. 2006;7:392–401.
- Stupp R, Mason WP, van den Bent MJ, Weller M, Fisher B, Taphoorn MJ, et al. Radiotherapy plus concomitant and adjuvant temozolomide for glioblastoma. *N Engl J Med*. 2005;352:987–996.
- Parato KA, Senger D, Forsyth PA, Bell JC. Recent progress in the battle between oncolytic viruses and tumours. *Nat Rev Cancer*. 2005;5:965–976.
- Everts B, van der Poel HG. Replication-selective oncolytic viruses in the treatment of cancer. *Cancer Gene Ther*. 2005;12:141–161.
- Lun X, Senger DL, Alain T, Oprea A, Parato K, Stojdl D, et al. Effects of intravenously administered recombinant vesicular stomatitis virus (VSV(deltaM51)) on multifocal and invasive gliomas. *J Natl Cancer Inst*. 2006;98:1546–1557.
- Ozduman K, Wollmann G, Piepmeier JM, van den Pol AN. Systemic vesicular stomatitis virus selectively destroys multifocal glioma and metastatic carcinoma in brain. *J Neurosci*. 2008;28:1882–1893.
- Rommelaere J, Cornelis JJ. Autonomous parvoviruses. In: Hernáiz Driever, P, Rabkin, SD eds. *Replication-Competent Viruses for Cancer Therapy Monographs in Virology*. Vol 22. Basel: Karger; 2001:100–129.
- Cornelis J, Deleu L, Koch U, Rommelaere J. Parvovirus oncosuppression. In: Kerr, JR, Cotmore, SF, Bloom, ME, Linden, RM, Parrish, CR, eds. *The Parvoviruses*. London: Hodder Arnold 2006;365–384.
- Cornelis JJ, Chen YQ, Spruyt N, Duponchel N, Cotmore SF, Tattersall P, et al. Susceptibility of human cells to killing by the parvoviruses H-1 and minute virus of mice correlates with viral transcription. *J Virol*. 1990;64:2537–2544.
- Cornelis JJ, Becquart P, Duponchel N, Salome N, Avalosse BL, Namba M, et al. Transformation of human fibroblasts by ionizing radiation, a chemical carcinogen, or simian virus 40 correlates with an increase in susceptibility to the autonomous parvoviruses H-1 virus and minute virus of mice. *J Virol*. 1988;62:1679–1686.
- Chen YQ, Tuynder MC, Cornelis JJ, Boukamp P, Fusenig NE, Rommelaere J. Sensitization of human keratinocytes to killing by parvovirus H-1 takes place during their malignant transformation but does not require them to be tumorigenic. *Carcinogenesis*. 1989;10:163–167.
- Bashir T, Horlein R, Rommelaere J, Willwand K. Cyclin A activates the DNA polymerase delta-dependent elongation machinery in vitro: a parvovirus DNA replication model. *Proc Natl Acad Sci USA*. 2000;97:5522–5527.
- Di Piazza M, Mader C, Geletneký K, Herrero YCM, Weber E, Schlehofer J, et al. Cytosolic activation of cathepsins mediates parvovirus H-1-induced killing of cisplatin and TRAIL-resistant glioma cells. *J Virol*. 2007;81:4186–4198.
- Le Cesne A, Dupressoir T, Janin N, Spielmann M, Le Chevalier T, Sancho-Garnier H, et al. Intra-lesional administration of a live virus, parvovirus H-1 (PVH-1) in cancer patients: a feasibility study. *Proc Annu Meet Am Soc Clin Oncol*. 1993;12:297.
- Toolan HW, Saunders EL, Southam CM, Moore AE, Levin AG. H-1 virus viremia in the human. *Proc Soc Exp Biol Med*. 1965;119:711–715.
- Herrero YCM, Cornelis JJ, Herold-Mende C, Rommelaere J, Schlehofer JR, Geletneký K. Parvovirus H-1 infection of human glioma cells leads to complete viral replication and efficient cell killing. *Int J Cancer*. 2004;109:76–84.
- Aas AT, Brun A, Blennow C, Stromblad S, Salford LG. The RG2 rat glioma model. *J Neurooncol*. 1995;23:175–183.
- Rorden C, Brett M. Stereotaxic display of brain lesions. *Behav Neurol*. 2000;12:191–200.
- Gart JJ, Krewski D, Lee PN, Tarone RE, Wahrendorf J. The design and analysis of long-term animal experiments. In: IACR, ed. *Statistical Methods in Cancer Research*. Lyon: IARC; 1986.
- Wrzesinski C, Tesfay L, Salome N, Jauniaux JC, Rommelaere J, Cornelis J, et al. Chimeric and pseudotyped parvoviruses minimize the contamination of recombinant stocks with replication-competent viruses and identify a DNA sequence that restricts parvovirus H-1 in mouse cells. *J Virol*. 2003;77:3851–3858.
- Raykov Z, Balboni G, Aprahamian M, Rommelaere J. Carrier cell-mediated delivery of oncolytic parvoviruses for targeting metastases. *Int J Cancer*. 2004;109:742–749.
- Jacoby RO, Ball-Goodrich LJ, Besselsen DG, McKisic MD, Riley LK, Smith AL. Rodent parvovirus infections. *Lab Anim Sci*. 1996;46:370–380.
- Fueyo J, Alemany R, Gomez-Manzano C, Fuller GN, Khan A, Conrad CA, et al. Preclinical characterization of the antiglioma activity of a tropism-enhanced adenovirus targeted to the retinoblastoma pathway. *J Natl Cancer Inst*. 2003;95:652–660.
- Gromeier M, Lachmann S, Rosenfeld MR, Gutin PH, Wimmer E. Intergeneric poliovirus recombinants for the treatment of malignant glioma. *Proc Natl Acad Sci USA*. 2000;97:6803–6808.
- Lun X, Yang W, Alain T, Shi ZQ, Muzik H, Barrett JW, et al. Myxoma virus is a novel oncolytic virus with significant antitumor activity against experimental human gliomas. *Cancer Res*. 2005;65:9982–9990.
- Wilcox ME, Yang W, Senger D, Rewcastle NB, Morris DG, Brasher PM, et al. Reovirus as an oncolytic agent against experimental human malignant gliomas. *J Natl Cancer Inst*. 2001;93:903–912.
- Shah AC, Price KH, Parker JN, Samuel SL, Meleth S, Cassady KA, et al. Serial passage through human glioma xenografts selects for a Deltagamma134.5 herpes simplex virus type 1 mutant that exhibits decreased neurotoxicity and prolongs survival of mice with experimental brain tumors. *J Virol*. 2006;80:7308–7315.
- Kambara H, Okano H, Chiocca EA, Saeki Y. An oncolytic HSV-1 mutant expressing ICP34.5 under control of a nestin promoter increases survival of animals even when symptomatic from a brain tumor. *Cancer Res*. 2005;65:2832–2839.
- Mariani CL, Kouri JG, Streit WJ. Rejection of RG-2 gliomas is mediated by microglia and T lymphocytes. *J Neurooncol*. 2006;79:243–253.
- Raykov Z, Grekova S, Galabov AS, Balboni G, Koch U, Aprahamian M, et al. Combined oncolytic and vaccination activities of parvovirus H-1 in a metastatic tumor model. *Oncol Rep*. 2007;17:1493–1499.